# Supporting Information for "Probing microsecond time scale dynamics in proteins by methyl $^1$H CPMG relaxation dispersion NMR measurements. Application to activation of the signaling protein NtrC$^r$."

Renee Otten,[†] Janice Villali,[‡] Dorothee Kern,[‡] and Frans A. A. Mulder[*,†]

*Groningen Biomolecular Sciences and Biotechnology Institute, University of Groningen, Nijenborgh 4, 9747 AG Groningen, The Netherlands, and Department of Biochemistry and Howard Hughes Medical Institute, Brandeis University, Waltham, MA 02452, USA*

E-mail: f.a.a.mulder@rug.nl

The Supporting Information for "Probing microsecond time scale dynamics in proteins by methyl $^1$H CPMG relaxation dispersion NMR measurements. Application to activation of the signaling protein NtrC$^r$" consists of a detailed description of experimental scheme C, and the following tables and figures:

Figure S1 shows the CPMG relaxation dispersion profiles for calbindin $D_{9k}$ using the different experimental schemes and was used to validate the proposed methodology.

[*]To whom correspondence should be addressed
[†]University of Groningen
[‡]Brandeis University

Figure S2 shows the CPMG relaxation dispersion profiles for all methyl groups in NtrC$^r$ that exhibit an exchange contribution.

Table S1 contains the effective CPMG field strengths used for recording the CPMG relaxation dispersion profiles on NtrC$^r$.

Table S2 contains the the exchange parameters for all methyl groups in NtrC$^r$ showing an exchange contribution, obtained from fitting the $^1$H CPMG data from 600- and 800 MHz simultaneously on a per-residue basis.

# Description of the pulse sequences used to measure $^1$H CPMG relaxation dispersion experiments.

**Product Operator Formalism, scheme C (figure 1):** At point *A* in the pulse sequence the density operator is proportional to $C_X^M$ and will evolve under the one-bond $J_{CC}$ scalar coupling during CT/2 (= $1/2J_{CC}$ = 14 ms) to $2C_Y^M C_Z$ and is equal to -$2C_Z^M C_Y$ after the 90° carbon pulse (point *B*). In the subsequent INEPT period there will be evolution due to the one-bond $J_{CH}$ scalar coupling and at point *C* in the sequence the magnetization can be expressed as $4C_Z^M C_X H_Z$ or -$2C_Z^M C_Y$ depending if there is a proton attached or not, respectively. Phase-cycling of the 90° proton pulse with $\phi_4$ (between y and -y), not followed by the receiver, will eliminate the first term. At point *C* in the sequence, where the density operator is proportional to $2C_Y^M C_Z$, carbon chemical shift evolution will take place for CT/2 (= $1/2J_{CC}$) and the one-bond $J_{CH}$ scalar coupling is active for a period of $\kappa = 1/(2J_{CH})$. The density operator at point *D* is, therefore, equal to -$2C_Y^M H_Z^M$ and represents a coherence originating from methyl groups with a fully deuterated neighboring carbon.

**Detailed description of the results obtained with scheme C, figure 1:** It is obvious from Figures 4 and S1 that significant artifacts arise from the protonation at the $\gamma$1-position of Ile and $\beta$-position of Thr residues, but also that these can be purged by choosing experimental scheme C

(Figure 1). Using this pulse scheme, flat lines are obtained for Ile-$\delta$1 and Thr methyl groups as well (Figure 4, panels B and D), with an average RMSD value of $0.22 \pm 0.03$ s$^{-1}$ for the two Ile-$\delta$1 and one Thr of calbindin $D_{9k}$ considered here. Of note, the background $R_{2,\mathrm{eff}}$ obtained using scheme C is also lower (4.41 vs. 3.41 s$^{-1}$ for Ile-$\delta$1 and 4.83 vs. 4.09 s$^{-1}$ for Thr, respectively). This is expected, since also the $^1\mathrm{H} - {}^1\mathrm{H}$ dipolar interaction with the neighboring nuclei is removed in this case. In agreement with this observation, the absence of $^1\mathrm{H}^{\mathrm{N}} - {}^1\mathrm{H}^{\alpha}$ interaction in perdeuterated protein samples is shown to have the same effect.[1,2] A comparison between the curves obtained using schemes A and C (Figure 1) shows that the selection against protonation at the neighboring carbon does not lead to different results for Ala, Ile-$\gamma$2, Met, and Val methyl groups (<RMSD> = $0.26 \pm 0.06$ s$^{-1}$ versus $0.20 \pm 0.04$ s$^{-1}$), in accord with the high level of deuteration in these side chains. Consistent with this observation there is neither a significant difference in background $R_{2,\mathrm{eff}}$ for these methyl groups between the two experiments. Finally, it should be noted that in scheme C $\sim$14 ms is needed to evolve the $J_{CC}$ coupling, which cannot be used at the same time for chemical shift encoding. Therefore, the resolution of the resulting 2D spectra is a factor of two lower than for scheme A. Although one could increase the period for chemical shift evolution from $1/(2J_{CC})$ to $3/(2J_{CC})$ to obtain a higher resolution, at the cost of signal intensity, scheme C is only advantageous for Ile-$\delta$1 and Thr methyl groups, with the proposed labeling.

Of note, the background $R_{2,\mathrm{eff}}$ obtained using scheme C is also lower (4.41 vs. 3.41 s$^{-1}$ for Ile-$\delta$1 and 4.83 vs. 4.09 s$^{-1}$ for Thr, respectively). This is expected, since also the $^1\mathrm{H} - {}^1\mathrm{H}$ dipolar interaction with the neighboring nuclei is removed in this case. In agreement with this observation, the absence of $^1\mathrm{H}^{\mathrm{N}} - {}^1\mathrm{H}^{\alpha}$ interaction in perdeuterated protein samples is shown to have the same effect.[1,2] A comparison between the curves obtained using schemes A and C (Figure 1) shows that the selection against protonation at the neighboring carbon does not lead to different results for Ala, Ile-$\gamma$2, Met, and Val methyl groups (<RMSD> = $0.26 \pm 0.06$ s$^{-1}$ versus $0.20 \pm 0.04$ s$^{-1}$), in accord with the high level of deuteration in these side chains. Consistent with this observation there is neither a significant difference in background $R_{2,\mathrm{eff}}$ for these methyl groups between the two experiments.

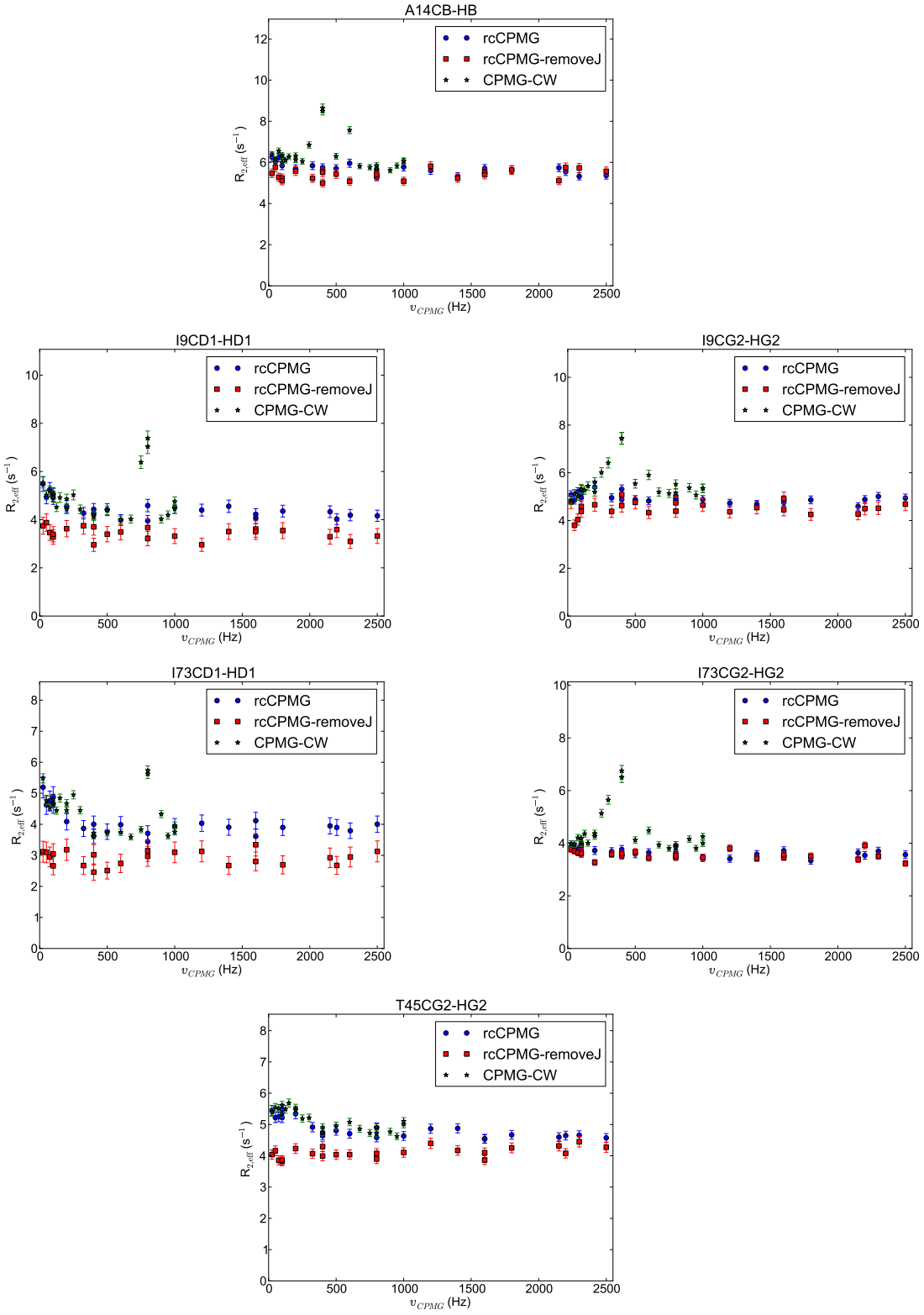


Figure S1: $^{1}$H CPMG relaxation dispersion profiles for all non-overlapping methyl groups of calbindin $D_{9k}$ measured at 600 MHz.

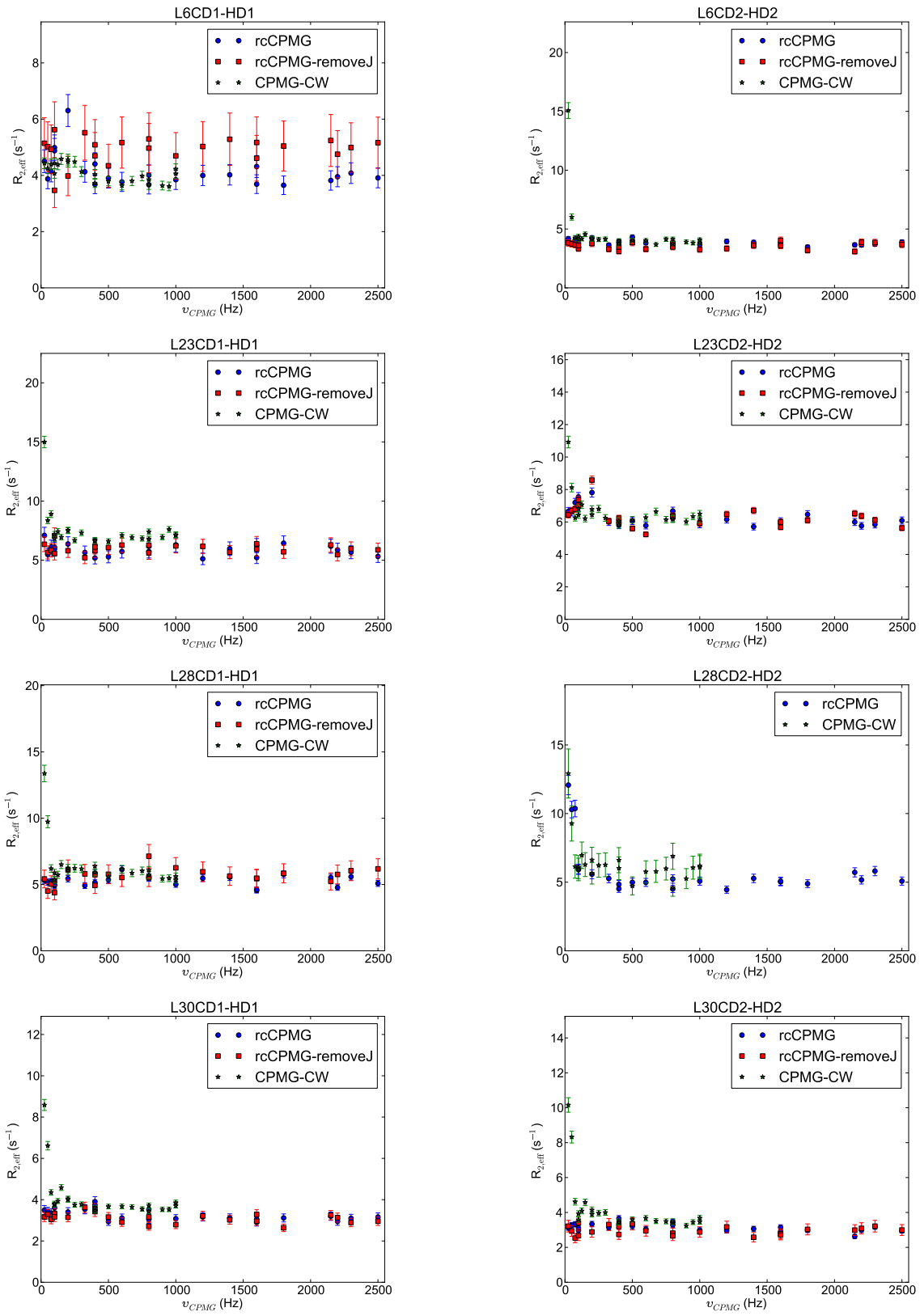


Figure S1: $^{1}$H CPMG relaxation dispersion profiles for all non-overlapping methyl groups of calbindin $D_{9k}$ measured at 600 MHz.

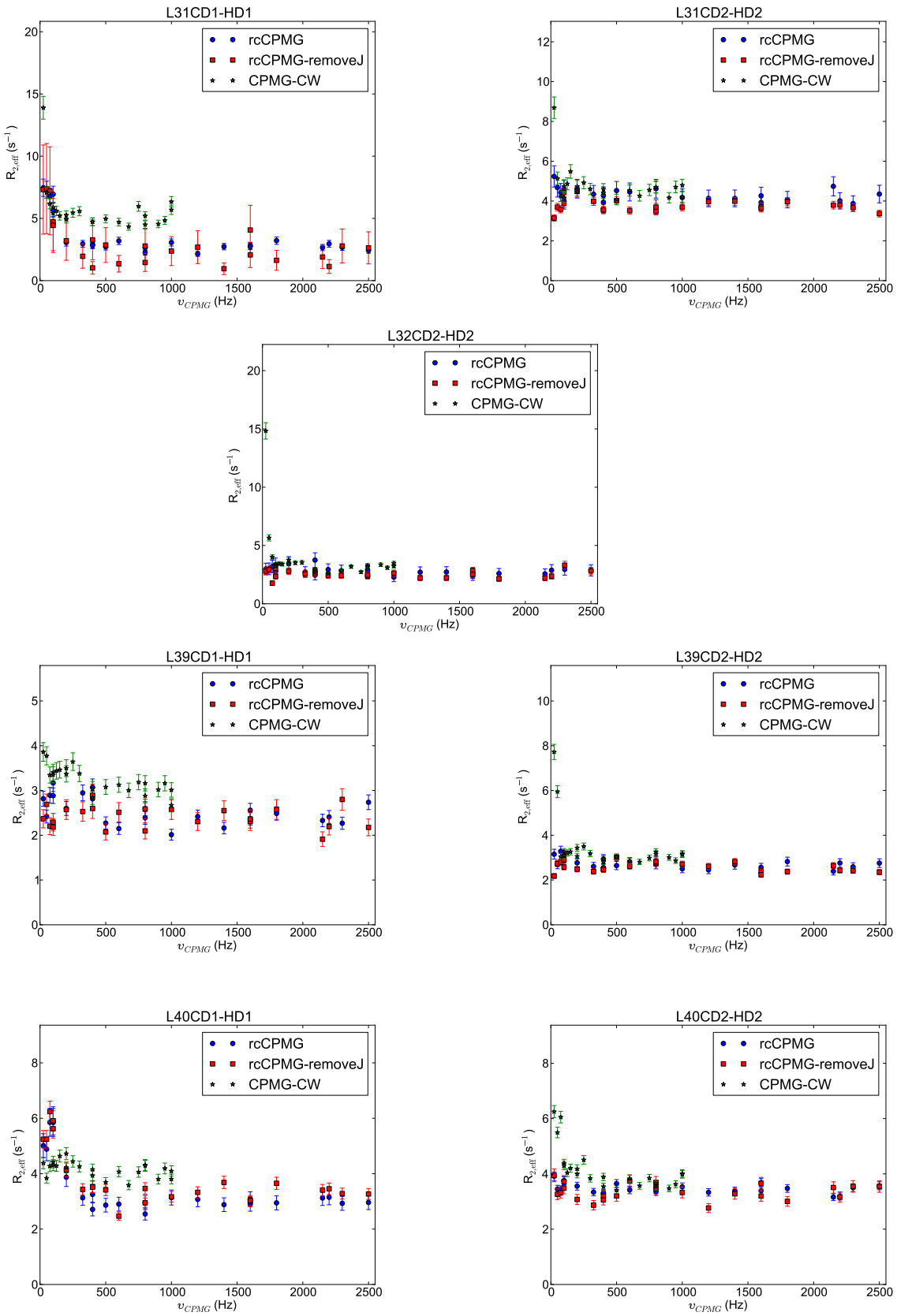


Figure S1: $^{1}$H CPMG relaxation dispersion profiles for all non-overlapping methyl groups of calbindin $D_{9k}$ measured at 600 MHz.

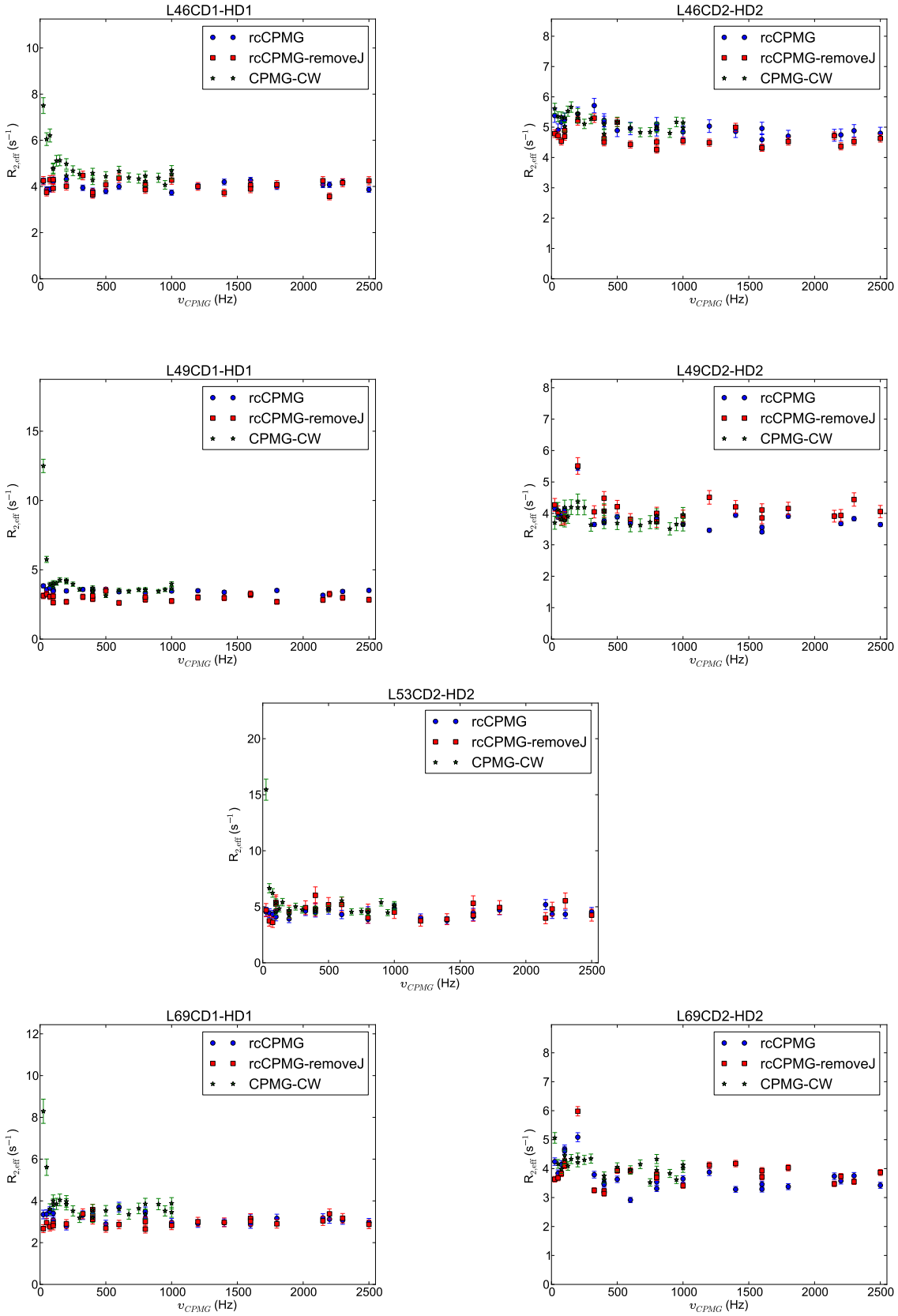


Figure S1: $^{1}$H CPMG relaxation dispersion profiles for all non-overlapping methyl groups of calbindin $D_{9k}$ measured at 600 MHz.

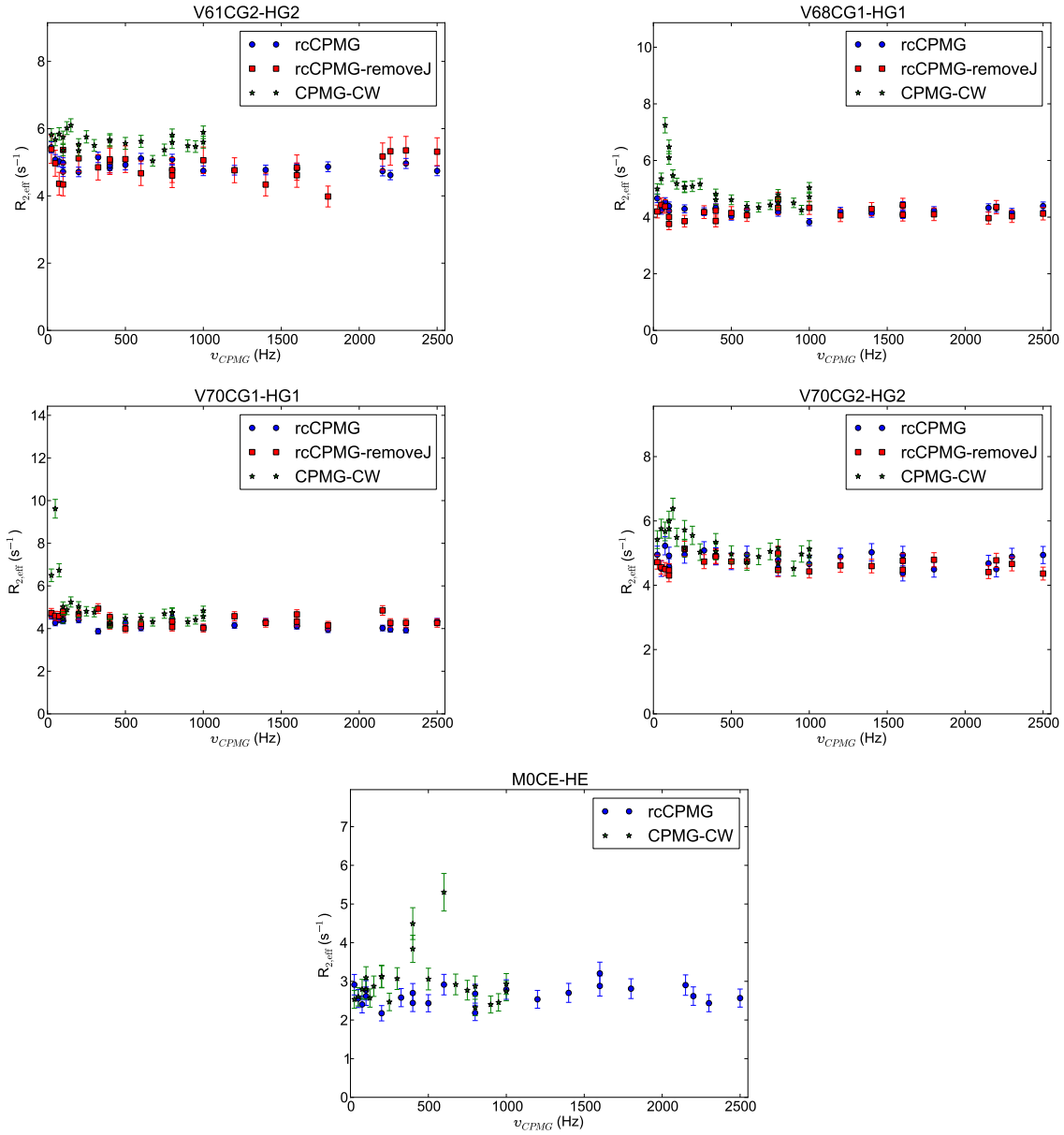


Figure S1: $^{1}$H CPMG relaxation dispersion profiles for all non-overlapping methyl groups of calbindin $D_{9k}$ measured at 600 MHz.

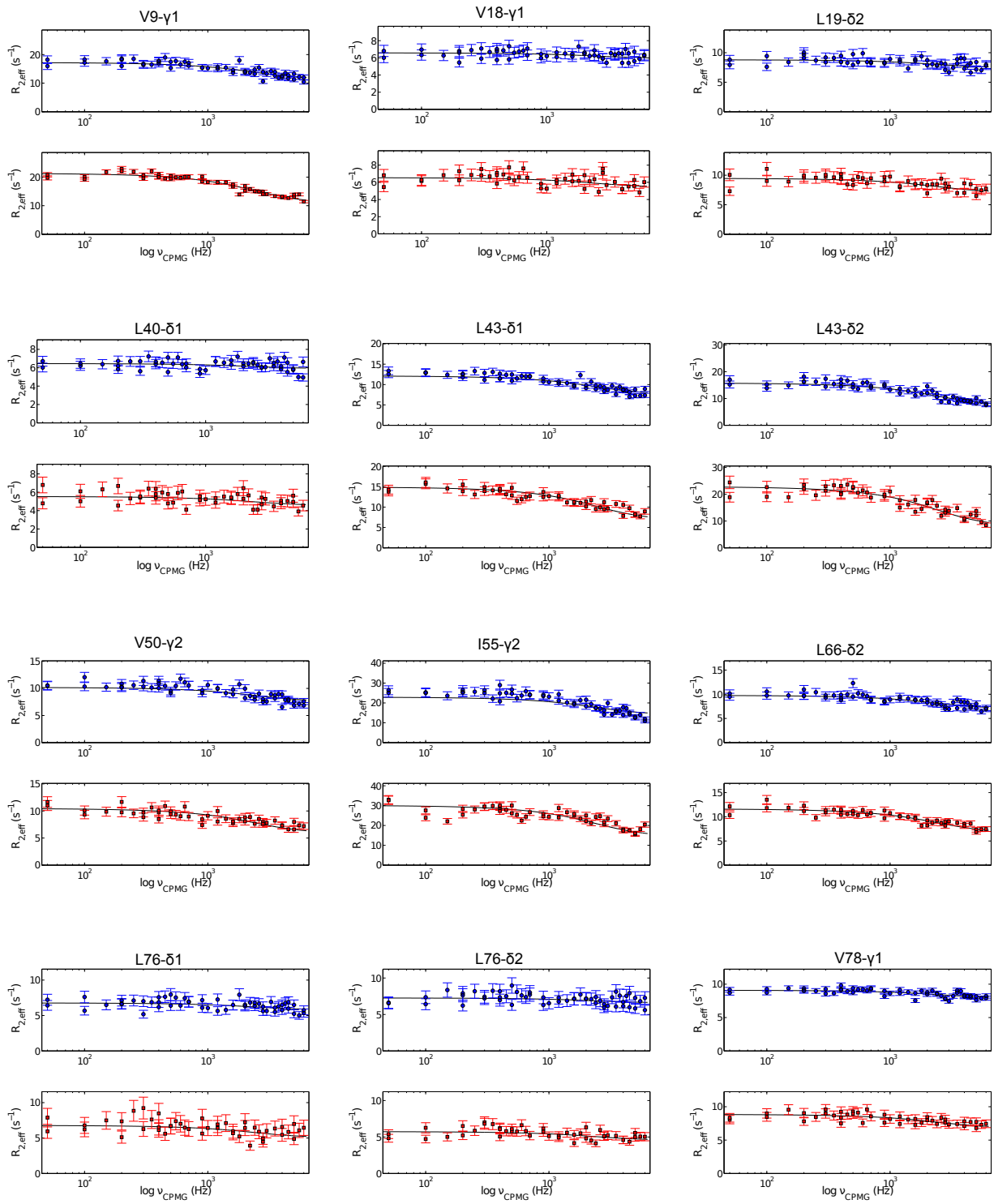


Figure S2: $^{1}$H CPMG relaxation dispersion profiles (measured at 600 and 800 MHz) for all methyl groups in NtrC$^{r}$ showing exchange. The solid lines correspond to the best curves, obtained from fitting the experimental data from both fields simultaneously to the appropriate two-site exchange equation using $\tau_{ex}$ = 15458 s$^{-1}$ determined from the global analysis of all profiles.

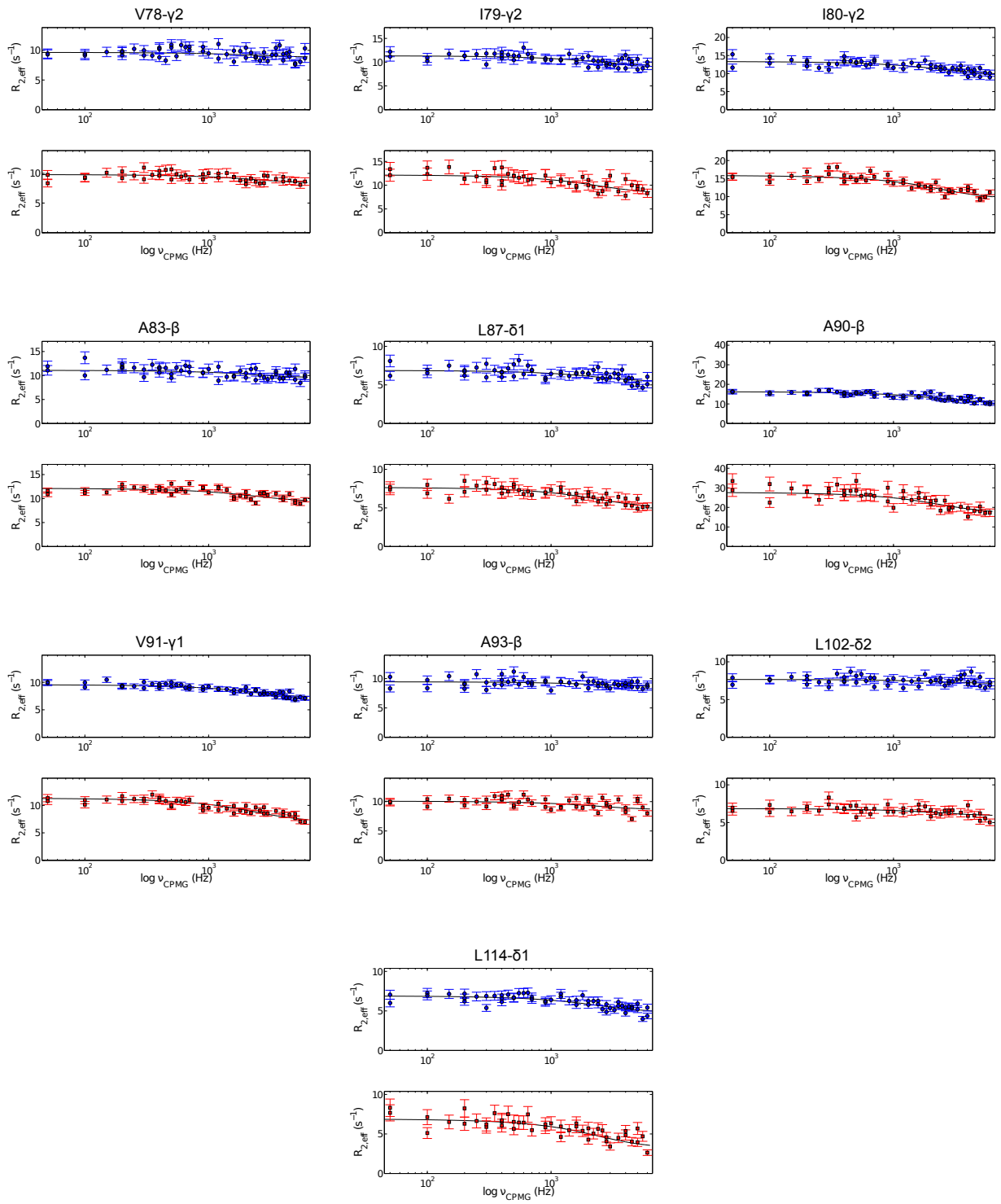


Figure S2: $^{1}$H CPMG relaxation dispersion profiles (measured at 600 and 800 MHz) for all methyl groups in NtrC$^{r}$ showing exchange. The solid lines correspond to the best curves, obtained from fitting the experimental data from both fields simultaneously to the appropriate two-site exchange equation using $\tau_{ex}$ = 15458 s$^{-1}$ determined from the global analysis of all profiles.

Table S1: Effective field strengths, $\nu_{CPMG}$, used in the $^1$H CPMG experiments of NtrC$^r$ measured at 600 and 800 MHz.

| magnetic field (MHz) | $\nu_{CPMG}$ (Hz) |
|---|---|
| 600 | 50 (2x), 100 (2x), 150, 200 (2x), 250, 300 (2x), 350, 400 (2x), 450, 500 (2x), 550, 600, 650, 700 (2x), 900 (2x), 1000, 1200 (2x), 1400, 1600 (2x), 1800, 2000 (2x), 2200, 2400 (2x), 2600, 2800 (2x), 3000, 3250, 3500 (2x), 3750, 4000 (2x), 4250, 4500 (2x), 5000 (2x), 5500, 6000 (2x) |
| 800 | 50 (2x), 100 (2x), 150, 200 (2x), 250, 300 (2x), 350, 400 (3x), 450, 500 (2x), 550, 600, 650, 700, 900 (2x), 1000, 1200 (2x), 1400, 1600 (2x), 1800, 2000 (2x), 2200, 2400, 2600, 2800 (2x), 3000, 3500, 4000 (2x), 4500 (2x), 5000 (2x), 5500, 6000 |

$\nu_{CPMG} = 1/(4\tau_c)$, where $2\tau_c$ is the interval between the 180° proton pulses during the CPMG element[3]

Table S2: Relaxation Dispersion Parameters for Methyl Groups in NtrC$^r$ at 25°C$^a$.

| methyl group | $\Phi_{ex}$ $10^4$ ($s^{-2}$) | $\delta\omega^b$ (ppm) | $\tau_{ex}$ ($\mu$s) | $p_B{}^c$ (%) | $R_{2,eff}$ ($\nu_{CPMG} \to \infty$)$^d$ ($s^{-1}$) | | $R_{ex}{}^d$ ($s^{-1}$) | | $\alpha^e$ | $\chi_v^{2\,f}$ |
|---|---|---|---|---|---|---|---|---|---|---|
| V9-$\gamma$1 | 7.5 ± 0.7 | - | 76.275 ± 5.729 | | 11.67 ± 0.22 | 11.44 ± 0.32 | 5.69 | 10.13 | | 1.48 |
| V18-$\gamma$2 | 1.5 ± 1.8 | - | 47.736 ± 37.667 | | 5.85 ± 0.35 | 5.24 ± 0.62 | 0.72 | 1.28 | | 0.86 |
| L19-$\delta$2 | 2.2 ± 1.2 | - | 62.275 ± 25.597 | | 7.41 ± 0.29 | 7.01 ± 0.52 | 1.38 | 2.45 | | 0.89 |
| L40-$\delta$1 | 137.7 ± 15307.2 | - | 4.338 ± 241.206 | | 0.47 ± 332.05 | -5.12 ± 590.56 | 5.97 | 10.62 | | 1.00 |
| L43-$\delta$1 | | 1.823 ± 0.000 | 110.391 ± 0.000 | 0.149 ± 0.000 | 7.62 ± 0.12 | 7.52 ± 0.01 | 4.93 | 6.83 | 1.13 | 1.03 |
| L43-$\delta$2 | 13.0 ± 1.8 | - | 64.978 ± 7.124 | | 7.34 ± 0.41 | 7.83 ± 0.72 | 8.45 | 15.02 | | 1.21 |
| V50-$\gamma$2 | | 2.624 ± 0.000 | 154.481 ± 38.659 | 0.070 ± 0.013 | 7.35 ± 0.00 | 6.17 ± 0.19 | 3.15 | 3.63 | 0.49 | 1.15 |
| I55-$\gamma$2 | | 3.241 ± 0.302 | 183.470 ± 65.036 | 0.275 ± 0.088 | 12.00 ± 0.84 | 13.87 ± 0.74 | 12.50 | 13.47 | 0.26 | 1.63 |
| L66-$\delta$2 | 3.8 ± 0.8 | - | 71.057 ± 12.052 | | 7.07 ± 0.21 | 6.85 ± 0.36 | 2.72 | 4.84 | | 0.96 |
| L76-$\delta$1 | 1.2 ± 0.8 | - | 79.172 ± 43.369 | | 5.87 ± 0.23 | 5.18 ± 0.43 | 0.93 | 1.65 | | 0.88 |
| L76-$\delta$2 | 0.7 ± 0.4 | - | 89.898 ± 42.835 | | 6.67 ± 0.16 | 4.69 ± 0.24 | 0.62 | 1.11 | | 0.86 |
| V78-$\gamma$1 | 1.4 ± 0.6 | - | 75.691 ± 23.912 | | 8.03 ± 0.15 | 6.96 ± 0.28 | 1.08 | 1.93 | | 1.07 |
| V78-$\gamma$2 | 2.0 ± 2.3 | - | 48.347 ± 36.964 | | 8.68 ± 0.45 | 8.06 ± 0.79 | 0.96 | 1.70 | | 0.93 |
| I79-$\gamma$2 | 2.3 ± 0.8 | - | 90.597 ± 26.768 | | 9.36 ± 0.25 | 8.65 ± 0.44 | 2.08 | 3.70 | | 0.75 |
| I80-$\gamma$2 | 6.1 ± 1.4 | - | 61.610 ± 10.110 | | 9.55 ± 0.32 | 9.10 ± 0.54 | 3.78 | 6.73 | | 1.23 |
| A83-$\beta$ | 3.3 ± 1.6 | - | 52.699 ± 17.210 | | 9.32 ± 0.34 | 8.98 ± 0.56 | 1.74 | 3.09 | | 1.38 |
| L87-$\delta$1 | 9.2 ± 11.0 | - | 27.073 ± 17.774 | | 4.30 ± 1.36 | 3.07 ± 2.42 | 2.49 | 4.43 | | 0.81 |
| A90-$\beta$ | 13.7 ± 4.0 | - | 49.375 ± 9.886 | | 9.33 ± 0.75 | 15.33 ± 1.39 | 6.76 | 12.02 | | 1.26 |
| V91-$\gamma$1 | 5.5 ± 1.7 | - | 49.735 ± 10.610 | | 6.78 ± 0.32 | 6.35 ± 0.57 | 2.72 | 4.84 | | 1.03 |
| A93-$\beta$ | 3.4 ± 4.8 | - | 34.484 ± 28.677 | | 8.24 ± 0.73 | 7.93 ± 1.29 | 1.18 | 2.09 | | 1.59 |
| L102-$\delta$1 | 138.6 ± 18327.1 | - | 4.349 ± 287.612 | | 1.62 ± 398.55 | -3.89 ± 708.83 | 6.03 | 10.72 | | 0.94 |
| L114-$\delta$2 | 7.0 ± 4.1 | - | 38.090 ± 14.035 | | 4.14 ± 0.64 | 1.99 ± 1.14 | 2.65 | 4.72 | | 1.20 |

[a] exchange parameters are obtained by fitting the dispersion profiles measured at 600 and 800 MHz simultaneously on a per-residue basis. The uncertainties in the paramters have been estimated using a Monte Carlo analysis. [b] in the case of fast exchange $\delta\omega$ was calculated assuming equal populations and, therefore, these values represent lower limits. For other populations ($p_C$ and $p_D$) the chemical shift difference can be calculated according to $\delta\omega_{CD} = \delta\omega_{AB}\sqrt{(p_A p_B / p_C p_D)}$. [c] population of the minor state. [d] first column $\omega_0/2\pi$ = 600 MHz and, second column $\omega_0/2\pi$ = 800 MHz. [e] values of $\alpha$ are calculated according to Millet *et al.*[4] and are only given in case of model 3; $0 < \alpha < 1$: slow exchange, $\alpha \sim 1$: intermediate exchange, $1 < \alpha < 2$: fast exchange. [f] the reduced $\chi^2$, $\chi_v^2$ is calculated using $\chi_v^2 = \chi^2/(N - m)$, where N is the number of experimental data points and m is the number of parameters.

## References


(1) Ishima, R.; Wingfield, P. T.; Stahl, S. J.; Kaufman, J. D.; Torchia, D. A. *J. Am. Chem. Soc.* **1998**, *120*, 10534–10542.

(2) Ishima, R.; Torchia, D. A. *J. Biomol. NMR* **2003**, *25*, 243–248.

(3) Mulder, F. A. A.; Skrynnikov, N. R.; Hon, B.; Dahlquist, F. W.; Kay, L. E. *J. Am. Chem. Soc.* **2001**, *123*, 967–975.

(4) Millet, O.; Loria, J. P.; Kroenke, C. D.; Pons, M.; Palmer, A. G. *J. Am. Chem. Soc.* **2000**, *122*, 2867–2877.